Postnatal Expansion, Maturation and Functionality of MR1T Cells in Humans

Gwendolyn M. Swarbrick[1,4¶*], Anele Gela[5¶], Meghan E. Cansler[1], Megan D. Null[1], Rowan B. Duncan[1], Elisa Nemes[5], Muki Shey[5, 6], Mary Nsereko[7], Harriet Mayanja-Kizza[7, 8], Sarah Kiguli[7, 9], Jeffrey Koh[3], Willem A. Hanekom[5], Mark Hatherill[5], Christina Lancioni[1], David M. Lewinsohn[2, 4], Thomas J. Scriba[5&], Deborah A. Lewinsohn[1&]

[1]Division of Infectious Diseases, Department of Pediatrics, Oregon Health & Science University, Portland, Oregon, USA

[2]Division of Pulmonary and Critical Care Medicine, Department of Medicine, Oregon Health & Science University, Portland, Oregon, USA

[3]Department of Anesthesiology and Perioperative Medicine, Oregon Health & Science University, Portland, Oregon, USA

[4]Portland Veterans Administration Healthcare System, Portland, Oregon, USA

[5]South African Tuberculosis Vaccine Initiative, Institute of Infectious Disease and Molecular Medicine and Division of Immunology, Department of Pathology, University of Cape Town, Cape Town, South Africa

[6]Department of Medicine & Wellcome Centre for Infectious Disease Research in Africa (CIDRI-Africa), Institute of Infectious Disease and Molecular Medicine, University of Cape Town, South Africa

[7]Uganda-CWRU Research Collaboration, Kampala, Uganda.

[8]Dept of Medicine, Makerere University, Kampala, Uganda.

[9]Dept of Paediatrics, Makerere University, Kampala, Uganda.

*Correspondence
Gwendolyn Swarbrick
swarbric@ohsu.edu

¶These authors contributed equally to this work.

&These authors are Joint Senior Authors.

Keywords: innate T cells, human mucosal immunology, MAIT cells, infant, tuberculosis.

Abstract

MR1-restricted T (MR1T) cells are a T cell subset that recognizes and mediates host immune responses to a broad array of microbial pathogens, including *Mycobacterium tuberculosis*. Here, we sought to characterize development of circulating human MR1T cells defined by MR1-5-OP-RU tetramer labelling and expression of TRAV1-2/CD26/CD161. We analysed postnatal expansion, maturation and functionality of peripheral blood MR1T cells in cohorts from three different geographic settings with different tuberculosis (TB) vaccination practices, levels of exposure to and infection with *M. tuberculosis.* Early after birth, frequencies of MR1-5-OP-RU tetramer-defined MR1T cells increased rapidly by several fold. This coincided with marked phenotypic changes, from a predominantly $CD4^+$ and TRAV1-2^- phenotype in neonates, to predominantly TRAV1-2^+CD8^+ MR1T cells that also expressed CD26 and CD161. We also observed that tetramer$^+$ MR1T cells that expressed TNF upon mycobacterial stimulation were very low in neonates, but increased ~10-fold in the first year of life. These functional MR1T cells in all age groups were MR1-5-OP-RU tetramer$^{+,}$ TRAV1-2^+ cells and expressed CD26 and CD161, markers that appeared to signal phenotypic and functional maturation of this cell subset. This age-associated maturation was also marked by the loss of naïve T cell markers on tetramer$^+$ TRAV1-2^+ MR1T cells more rapidly than tetramer$^+$TRAV1-2^- MR1T cells and non-MR1T cells. These data suggest that neonates have infrequent populations of MR1T cells with diverse phenotypic attributes; and that exposure to the environment rapidly and preferentially expands the MR1-5-OP-RU tetramer$^+$TRAV1-2^+ population of MR1T cells, which becomes the predominant population of functional MR1T cells early during childhood.

Introduction

MR1-restricted T (MR1T) cells, also known as mucosal-associated invariant T (Paul K Sue) cells, are a highly conserved population of T-cells that exhibit innate-like functions similar to those described for NKT cells. MR1T cells are defined by their recognition of metabolite antigens presented by the monomorphic MHC class 1-related molecule, MR1, the most highly conserved MHC class I related molecule in mammalian species (Harriff et al., 2018; Godfrey et al., 2019). MAIT cells, the predominant subset of MR1T cells, are also defined by a highly restricted T-cell-receptor (TCR) repertoire, comprising an invariant TCR α-chain (TRAV1.2-TRAJ33/20/12 in humans; TRAV1-TRAJ33 in mice) with a CDR3 of constant length paired with a limited number of Vβ segments (Vβ2/13 in humans; Vβ6/8 in mice) (Treiner et al., 2003; Martin et al., 2009; Reantragoon et al., 2013; Lepore et al., 2014). MAIT cells have been defined by different methods. Prior to availability of the MR1 tetramer, MAIT cells were defined by expression of TRAV1-2 and other phenotypic markers, like CD161 and CD26. Now the MR1 tetramer can also be more broadly used to define MR1T cells. In peripheral blood, MAIT cells defined by MR1 tetramer or phenotype are highly concordant in adults (Sharma et al., 2015). As we will show in this paper, the MR1 tetramer allows detection of a much broader repertoire of MR1Ts that are not only restricted to TRAV1-2^{+} (MAIT cells).

MR1T cell development is a stepwise process, with an intra-thymic selection followed by peripheral expansion. Koay *et al* reported a three-stage development pathway for mouse and human MR1T cell populations, where three populations of human MR1T precursors were defined based on differential expression of CD27 and CD161. The initial two stages of MR1-5-OP-RU tetramer^{+}TRAV1-2+CD161^{-} cells, which were either CD27- or CD27+, occurred in the thymus and these cells were low in the periphery. The more mature MR1 tetramer^{+}TRAV1-2^{+}CD161^{+}CD27^{+} cells, designated as stage 3, have been shown to represent only a small fraction of T cells but form a more abundant population in adult blood (Martin et al., 2009; Dusseaux et al., 2011; Koay et al., 2016). Such studies indicate that MR1T cell thymopoeisis is complemented by an important postnatal peripheral expansion and maturation, which was recently shown to be dependent upon acquisition of the intestinal microbiome (Constantinides et al., 2019; Legoux et al., 2019).

MR1T cells recognize microbial derived riboflavin (Vitamin B2) biosynthesis intermediate derivatives, such as 5-OP-RU (5-(2-oxopropylideneamino)-6-d-ribitylaminouracil) and a broad spectrum of microbes that synthesize riboflavin, including *S. aureus, E. coli, and C. albicans* (Gold et al., 2010; Kjer-Nielsen et al., 2012; Gold et al., 2013; Corbett et al., 2014; Meermeier et al., 2016). While 5-OP-RU was the first MR1 ligand defined, several other ligands have subsequently been defined, including additional riboflavin-derived ligands, including both stimulatory and inhibitory ligands (Meermeier et al., 2016; Harriff et al., 2018). Upon recognition of microbial antigens or activation through cytokine signaling, MR1T cells display immediate effector function by secreting inflammatory cytokines and cytotoxic molecules, which can kill infected cells (Gold et al., 2010; Dusseaux et al., 2011; Le Bourhis et al., 2013; Kurioka et al., 2015). In a mouse model of pulmonary legionella infection, MR1T cells exhibited enhanced protection in an MR1-dependent manner, mediated by the effector molecules IFN-γ and GM-CSF (Wang et al., 2018). MR1T cells have also been shown to facilitate control of *Klebsiella pneumonia, Mycobacterium*

90 *bovis* BCG, and *Francicella tularensis* infections (Georgel et al., 2011; Meierovics et al., 2013;
91 Sakala et al., 2015; Meierovics and Cowley, 2016). Many of the bacterial pathogens that are
92 important causes of infant morbidity and mortality, including *S. aureus*, *S. pneumoniae*, and enteric
93 pathogens (e.g. *E. coli*, *Klebsiella*, *Salmonella*), are recognized by MR1T cells. MR1T cells
94 possess immediate innate-like, effector functions, and can therefore mediate immune functions
95 before priming, clonal expansion and maturation of antigen-specific MHC-restricted T cells.
96 Therefore, MR1T cells could play an important role in host defense to bacterial pathogens,
97 especially in infancy.

98 MR1T cells are known to also recognize and respond to *Mycobacterium tuberculosis,* the
99 leading global cause of mortality from a single infectious agent. Infants and young children suffer
100 disproportionately from disseminated and severe forms of tuberculosis (TB) disease and are
101 significantly more susceptible to disease than adults (Marais et al., 2004a; Marais et al., 2004b;
102 Marais et al., 2006). Here, we sought to characterize development of MR1T cells (defined by MR1-
103 tetramer labeling) and their subset of phenotypically defined MAIT cells (TRAV1-
104 $2^{+}CD26^{+}CD161^{+}$ T cells) by analyzing postnatal expansion, maturation and functionality in
105 humans. We compared MR1T/MAIT cell development in cohorts from three different settings
106 with differing TB vaccination practices and levels of exposure and infection with *M. tuberculosis.*

Results

Human participants

We enrolled nine cohorts across three different countries to study MR1T cell development. The cohorts in South Africa (SA) were neonates (cord blood, *n* = 10), infants (aged 10 weeks, BCG vaccinated at birth, *n* = 10) and adolescents [aged 14-18 years, BCG vaccinated at birth, QuantiFERON-TB Gold (QFT)-negative, *n* = 10]. The cohorts enrolled in the United States (US) were neonates (cord blood, *n* = 10), infants (aged 9-15 months, BCG unvaccinated, *n* = 10) and adults (aged 29-60 years, *n* = 10). The cohorts in Uganda (UG) were infants [2-24 months old, BCG vaccinated at birth +/-, tuberculin skin test (TST) +/-, *n* = 36], children (24 - 60 months, BCG vaccinated at birth +/-, TST +/-, *n* = 23) and adults (aged 18-60 years, BCG vaccinated at birth +/-, TST +/-, *n* = 91).

Frequencies of tetramer-defined MR1T cell and phenotypically-defined MAIT cell populations increase with age irrespective of BCG vaccination

We defined MR1T cells as $CD3^+$ T cells positively labeled with the MR1-5-OP-RU tetramer. MR1/6FP tetramers were used as a negative control. The MR1T cell subset, MAIT cells, were defined phenotypically as $CD3^+$ T cells that stained positive for antibodies against TRAV1-2, CD161 and CD26. This phenotypic definition of MAIT cells is concordant with the vast majority of tetramer-defined MR1T cells in adults (Sharma et al., 2015). We determined frequencies of MR1T cells and the phenotypically-defined MAIT cell subset in all cohorts (Fig 1). Because of limited availability of the MR1-5-OP-RU tetramer, determination of tetramer-defined MR1T cell frequencies in the Ugandan cohorts was performed on a subset of 10 donors (Fig 1B and S1 Fig). In all cohorts, both tetramer-defined MR1T cell and phenotypically-defined MAIT cell frequencies increased with age (Fig 1B).

Tetramer-defined MR1T cell and phenotypically-defined MAIT cell populations are concordant in adults, adolescents and infants but discordant in neonates

We next determined the degree of concordance between tetramer-defined MR1T cell and phenotypically-defined MAIT cell populations. The majority of phenotypically-defined MAIT cells population, defined by TRAV1-$2^+CD26^+CD161^+$ co-expression, also stained with MR1 tetramer in infants, adolescents and adults, demonstrating high concordance between tetramer-defined MR1T cells and phenotypically-defined MAIT cells in these cohorts. (Fig 1C). However, in cord blood from both SA and US neonates, these two populations were discordant as the minority of TRAV1-$2^+CD26^+CD161^+$ MAIT cells also expressed the MR1T tetramer (Fig 1C). The expression of CD4 and CD8 across the discordant, phenotypically-defined MAIT cell populations that do not bind MR1 tetramer cell populations varied between cohorts.

The MR1-5-OP-RU tetramer$^+$ subset of phenotypically-defined MAIT cells contain the functional population

To investigate whether tetramer-defined MR1T cells and phenotypically-defined MAIT cells have different functional capacity, we measured TNF expression in the US cohort by intracellular cytokine staining (ICS) and flow cytometry following incubation with *M. smegmatis*-infected A549 cells. Among all phenotypically defined by TRAV1-$2^+CD26^+CD161^+$ MAIT cells, only the MR1/5-OP-RU tetramer$^+$ subset expressed TNF; MR1-5-OP-RU tetramer-negative cells,

148 by contrast, did not appear to respond to *M. smegmatis* stimulation (Fig 2). Because of this result,
149 we focused on the functional, tetramer-defined MR1T cells for subsequent experiments.

150 **Neonates have higher proportions of CD4$^+$ and TRAV1-2$^-$ MR1T populations compared to**
151 **infants, adolescents and adults**

152 To explore the diversity of MR1T cells and how this may change during early development,
153 we applied the dimensionality reduction method, t-distributed stochastic neighbor embedding
154 (tSNE), on tetramer-defined MR1T cells. Five discrete phenotypic MR1T cell clusters were
155 identified in both the SA and US cohorts (Figure 3A-D), the relative proportions of which varied
156 with age (Figure 3B and D). Specifically, the CD4$^+$ (Clusters 3 and 4) and TRAV1-2$^-$CD26$^-$
157 CD161$^-$ (Clusters 1, 2 and 3) MR1T cell clusters predominated in neonates, while CD4$^-$CD8$^{+/-}$
158 TRAV1-2$^+$CD26$^+$CD161$^+$ cluster (Cluster 5) was predominant in infant, adolescent, and adult
159 cohorts from both the US and SA (Figure 3B and D). Relative proportions of MR1T cell clusters
160 in 10 week old (SA) and 12 month old (US) infants were more similar to those in adults and
161 adolescents than to those in neonates, consistent with the hypothesis that MR1T cells mature
162 rapidly upon exposure to MR1T cell antigens (Figure 3E and F). It was also noteworthy that CD4$^-$
163 CD8$^{+/-}$TRAV1-2$^+$CD26$^+$CD161$^+$ MR1T cells that fell into cluster 5 comprised a much lower
164 percentage of the MR1Ts in cord blood, while forming the dominant phenotype in 12-month-old
165 (US) infants. In the 10 week old (SA) infants, this cluster had started to appear but was not yet
166 "fully developed", suggesting rapid development during the first months of life, from a
167 predominantly TRAV1-2 negative to a TRAV1-2 positive population with loss of expression of
168 CD4 and acquisition of CD26 and CD161. We also note that in the US cohort only there is a
169 population that is positive for all markers. Because it was only seen in one cohort, it was excluded
170 from the comparison of clusters.

171 **MR1T cells become more functional with age**

172 Next, we explored how tetramer-defined MR1T cells developed functionally with age in
173 the US cohort by tracking the TNF-expressing population following *M. smegmatis* or
174 PMA/Ionomycin stimulation. TNF-expressing tetramer$^+$ MR1T cells in neonates were present at
175 very low frequencies (Figure 2B) and represented a much smaller proportion of the total tetramer$^+$
176 MR1T cell population than in infants and adults (Figure 4A and B). Proportions of tetramer$^+$ MR1T
177 cells responding to either mycobacteria or PMA/Ionomycin were higher in infants than adults
178 ($p=0.0007$ and $p=0.0021$, respectively) or neonates ($p<0.0001$ for both stimulations). However,
179 because tetramer$^+$ MR1T cell frequencies were higher in adults than infants (Figure 1B), overall
180 frequencies of TNF-producing MR1T cells were highest in adults. To explore the functional
181 capacity of MR1T cells relative to other T cell subsets within each cohort, we compared
182 proportions of TNF-expressing MR1T cells (CD3$^+$TCRγδ$^-$MR1-5-OP-RU$^+$) with TCRγδ T cells
183 (CD3$^+$TCRγδ$^+$ MR1-5OPRU$^-$), CD4$^+$ T cells (CD3$^+$TCRγδ$^-$MR1-5OPRU$^-$CD4$^+$) and CD8$^+$ T cells
184 (CD3$^+$TCRγδ$^-$MR1-5OPRU$^-$CD4$^+$) after PMA/Ionomycin stimulation (Figure 4C). In neonates,
185 proportions of TNF-expressing MR1T cells were significantly higher than proportions of TCRγδ
186 T cells and CD8$^+$ T cells. In infants and adults, proportions of TNF-expressing MR1T cells were
187 significantly higher than TCRγδ$^+$, CD4$^+$ and CD8$^+$ T cells (Figure 4C).

188 **Functional CD3$^+$MR1-5-OP-RU$^+$ MR1T cells are TRAV1-2$^+$**

189 Next, we investigated TRAV1-2 expression among functional, TNF-expressing
190 CD3$^+$MR1-5-OP-RU$^+$ MR1T cells. Only TRAV1-2$^+$ MR1 T cells produced TNF in response to
191 mycobacterial stimulation while TRAV1-2$^-$ MR1 T cells were not functional (Figure 4D). This
192 pattern was unique to mycobacterial stimulation since TNF-expressing TRAV1-2$^-$ MR1T cells
193 were observed in response to PMA/Ionomycin stimulation, particularly in infants and adults
194 (Figure 4E). Interestingly, the vast majority of these functional, TNF-expressing TRAV1-2$^+$
195 MR1T cells also expressed the phenotypic markers, CD26 and CD161 (Figure 4F-G). Thus, the
196 CD3$^+$MR1-5-OP-RU$^+$TRAV1-2$^+$CD26$^+$CD161$^+$ MR1T cell population contains the functional
197 MR1T cells that respond to mycobacteria. The frequency of this population increases very quickly
198 with age.

199 **TRAV1-2$^+$ MR1T cells lose naïve markers more rapidly with age than TRAV1-2$^-$ MR1T cells**
200 **or non-MR1T cells**

201 To characterize the development of MR1T cells further, we also measured expression of
202 CD27 and CD161, markers previously described to indicate MR1T cell maturation, and CD45RA,
203 CCR7, CD38 and CD56 on tetramer-defined MR1Ts (Figures 5-6) (Koay et al., 2018). A
204 population of immature MR1T cells, defined as CD27$^+$CD161$^-$ cells, was observed in neonates but
205 not in infants and adults, as previously described (Koay et al., 2016). This was also reflected by
206 expression of the more traditional T cell maturation markers, CD45RA, CCR7 and CD38 (Figure
207 6 A, C, E). Most tetramer-defined MR1T cells in neonates displayed a CD45RA$^+$CCR7$^+$CD38$^+$
208 "naïve" phenotype, but this phenotype was lost more rapidly with age on TRAV1-2$^+$ MR1Ts than
209 on TRAV1-2$^-$ MR1T cells or non-MR1T cells (Figure 6A-F). The inverse was true for the
210 activation marker, CD56, which was increased in neonatal, infant and adult TRAV1-2$^+$ tetramer-
211 defined MR1T cells compared to TRAV1-2$^-$ tetramer-defined MR1T cells and non-MR1T cells
212 (Figure 6G-H). These results are consistent with our finding that TRAV1-2$^+$ tetramer-defined
213 MR1T cells display functional capacity in all age groups, even though they represent the minority
214 of neonatal MR1T cells.

215 **Discussion**

216 We characterized the development of MR1T cells during early childhood in three cohorts,
217 two from Africa and one in the USA, to elucidate phenotypic and functional changes that occur
218 after birth and during the first few years of life. A better understanding of MR1T cell development
219 is critical given the likely role of MR1T cells as innate-like effectors that act as key mediators of
220 immunity in newborns, who are at very high risk of infection, including *M. tuberculosis.* We found
221 that neonates had relatively low frequencies of MR1T cells with high phenotypic diversity, which
222 included considerable proportions of $CD4^+$ and TRAV1-2^- cells. These patterns changed as early
223 as 10 weeks after birth, and became more prominent at 1-2 years of age, adolescence and ultimately
224 by adulthood. This included higher frequencies of MR1T cells in peripheral blood, characterized
225 by a preferential expansion in TRAV1-2^+CD8^+ MR1T cells such that TRAV1-2^+CD8^+MR1T cells
226 constituted the vast majority of the $tetramer^+$ MR1T cell population. The development also
227 included changes in expression of maturation markers and MR1T cell effector function, since
228 MR1T cells from older individuals had lower expression of the naïve T cell markers, CD45RA,
229 CCR7 and CD38, and an increased ability to express TNF.

230 Our finding that MR1T cells are found at low frequency in cord blood and increase in
231 frequency with age confirms our previous observations, as well as those of others, who have
232 utilized either the MR1-5-OP-RU tetramer or phenotypic characterization of MAIT cells to
233 demonstrate the expansion of these cell populations from birth through adulthood (Martin et al.,
234 2009; Gold et al., 2013; Walker et al., 2014; Koay et al., 2016; Ben Youssef et al., 2018; Gherardin
235 et al., 2018). The very rapid changes in MR1T cells seen after birth are striking and were clearly
236 seen in both African and American settings. This finding rules out the possibility that BCG
237 substantially contributes to these changes, since BCG is not routinely administered at birth in the
238 USA. Rather, it is more likely that changes occur upon the transition from the limited microbial
239 exposure in the womb to the postnatal environment, accompanied by the rapid colonization of the
240 gut microbiome. MR1T cells are absent in germ-free mice and depend on the colonization of the
241 gut microbiome with normal intestinal flora, which produce riboflavin (Le Bourhis et al., 2013;
242 Harriff et al., 2018; Legoux et al., 2019). We suggest that this colonization of the gut microbiome
243 is the driving force that accounts for the increase and phenotypic changes in MR1T cells in blood
244 after birth and the gain in functional capacity.

245 While we confirm our previous work that phenotypic definition of MAIT cells accurately
246 identifies functional MR1T cells in adults, we find that there is a high level of discordance in
247 neonates in part due to MR1-5-OP-RU $tetramer^+$ cells that do not express TRAV1-2, CD26 or
248 CD161. These cells are by definition MR1-restricted T cells as they bind the MR1-5-OP-RU
249 tetramer. However, these cells are poorly reactive to mycobacteria, suggesting that they either
250 recognize a different antigen or represent immature MR1T cells. The poor PMA/Ionomycin-
251 induced TNF secretion of these cells supports the latter. However, because our only measure of
252 MR1T cell responses was TNF-α production, we may have failed to detect other responses
253 characterized by the production of alternative cytokines or cytolytic markers.

254 We also show that neonates possess MR1-5-OP-RU $tetramer^-$ cells that phenotypically
255 resemble MAIT cells (the discordant MR1-5-OP-RU $tetramer^-$ phenotypically defined ($CD26^+$,
256 $CD161^+$, and TRAV1-2^+) MAIT cell population). As Fergusson *et al* suggested that distinct T

257 subsets that express CD161 share a common transcriptional profile characteristic of typical MR1T
258 cells (Fergusson et al., 2014), it is certainly possible that these CD161$^+$ cells are MR1-restricted or
259 share common attributes with MR1T cells. Further characterization of this neonatal T cell
260 population is required to determine whether or not these cells are indeed MR1-restricted and if so,
261 if these cells are immature or recognize distinct microbes, or produce a different cytokine not
262 detected in our functional assay. Given that, in the mouse model, 5-OP-RU produced by the
263 microbiome is necessary and sufficient to drive the expansion of typical MR1T cells (Legoux et
264 al., 2019), it is perhaps expected that with age tetramer-positive MR1T TRAV1-2$^+$ cells would
265 quickly become the predominant MR1T cell population, while tetramer negative MR1T cells
266 might persist as a minority population of naïve T cells.

267 Consistent with our prior findings (Gold et al., 2013) and those of Youssef *et al*. (Ben
268 Youssef et al., 2018), our phenotypic analysis of MR1-5-OP-RU tetramer$^+$ cells in neonates
269 demonstrates that MR1T cells expressed a naïve cell surface phenotype (CD45RA$^+$CCR7$^+$CD38$^+$)
270 and included a prominent subset of CD4$^+$ cells. It is noteworthy that these MR1T cells rapidly
271 lost expression of CD45RA, CCR7 and CD38 and acquired a phenotype consistent with those
272 observed in antigen-experienced memory T cells much more rapidly than other types of T cells
273 (Chua et al., 2012; Tsukamoto et al., 2013; Lindestam Arlehamn et al., 2014).

274 While Koay *et al* showed the functional potential of neonatal MR1T cells that produced
275 TNF following stimulation with PMA/Ionomycin, we show for the first time the presence of
276 functional microbe-reactive MR1T cells in neonates, albeit at low frequency. Virtually all of the
277 mycobacteria-reactive TNF-producing MR1T cells were contained within the TRAV1-2$^+$CD26$^+$
278 CD161$^+$ subset of 5-OP-RU tetramer$^+$ cells, which are also concordant with "Stage 3" MR1T cells
279 defined by Koay *et al*. Although the immature CD4$^+$, CD4-CD8- and/or TRAV1-2- MR1T cells
280 were maintained through to adulthood, we observed that CD8$^+$TRAV1-2$^+$ MR1T cells expanded
281 preferentially over TRAV1-2$^-$ MR1T cells. This expansion coincided with the acquisition of CD26
282 and CD161 as markers of mature functional MR1 T cells. In addition, we show that the frequency
283 of these functional mycobacterial-reactive MR1T cells increases ~10-fold in the first year of life.
284 A surprising finding was that given a comparable stimulus (PMA/Ionomycin and *M. smegmatis*),
285 the infant MR1Ts exhibited a higher functional capacity than the adults. Interestingly, we
286 demonstrated that relative to other T cell subsets, MR1T cells had the highest capacity to secrete
287 the pro-inflammatory cytokine, TNF-α, in infants. Thus, MR1T cells may represent an important
288 source of pro-inflammatory effectors in infants, who are more vulnerable to serious bacterial
289 infections in the first two years of life, relative to older children and adults.

290 Regarding newborns, it is not known to what degree the naïve phenotype and low
291 functionality of MR1T cells contributes to the very high susceptibility to bacterial infection in the
292 first two months of life (Paul K Sue, 2018). Since MR1T cells recognize important childhood
293 bacterial pathogens, including *S. aureus, S. pneumoniae and enteric pathogens (e.g. E. coli,*
294 *Klebsiella, Salmonella species*, it is plausible that the low frequency of functional MR1T cells
295 during the neonatal period contributes to neonatal susceptibility to infection. At the very least, our
296 findings add to the well-described differences in adaptive and innate immunity between neonates
297 and adults (Paul K Sue, 2018).

298 With regard to *M. tuberculosis*, there is mounting evidence that supports an important host
299 defense role for MR1T cells, especially during early infection. Upon encounter with
300 mycobacterial-infected cells, MR1T cells produce pro-inflammatory cytokines such as IFN-γ and
301 TNF (Gold et al., 2010), known to be essential mediators to host defense against *M. tuberculosis*
302 (Lindestam Arlehamn et al., 2014). MR1-deficient mice control BCG less well than wild type
303 mice (Chua et al., 2012). In humans, MR1 polymorphisms are associated with susceptibility to TB
304 meningitis (Seshadri et al., 2017). It is tempting to speculate, in light of the high susceptibility of
305 infants to TB, and the phenotypic and functional attributes of MR1T cells we observed, that MR1T
306 cells contribute to control of early infection with *M. tuberculosis* through their early and robust
307 anti-mycobacterial response, particularly in the lung.

Methods

Study participants

University of Cape Town, Western Cape, South Africa. All participants were enrolled either at the South African Tuberculosis Vaccine Initiative Field Site, Well-Baby Clinics or Maternity Wards in the Worcester region, near Cape Town, South Africa. Pregnant mothers were enrolled for collection of cord blood immediately after childbirth by Cesarean section. Mothers who may have been exposed to *M. tuberculosis*, HIV infected, had any other acute or chronic disease, and receiving medication other than anesthetic given during delivery were excluded. Infants born to HIV negative mothers, and who had received BCG at birth, had no perinatal complications, or household contact with any person with TB, and did not have any acute or chronic disease were enrolled for collection of blood. Healthy adolescents of 12-18 years of age without evidence of latent Mtb infection as determined by positivity negativity for the Tuberculin Skin Test (<10mm) or QuantiFERON (<0.35IU/mL) were enrolled for blood collection. Heparinized blood was collected for cord blood mononuclear cell (CBMC) and peripheral blood mononuclear cells (PBMC) isolation by means of density gradient centrifugation.

Oregon Health and Science University, Portland, OR, USA. Umbilical cord blood was obtained from the placenta of uncomplicated term pregnancies after delivery into citrate CPT tubes (BD). Blood was processed per manufacturer's instructions within 24hr of collection, and resulting CBMC cryopreserved. Infants aged 1-24 months undergoing elective surgery at OHSU Doernbecher Children's Hospital were enrolled. Infants had not received BCG vaccination, which is not part of the childhood immunization series in the United States. Blood was drawn into citrate CPT tubes (BD) and processed per manufacturer's instructions to isolate PBMC within 24hr of collection, and PBMC subsequently cryopreserved. Adult PBMC were obtained by leukapheresis from healthy adult donors and cryopreserved. Adult participants lacked any detectable responses to *Mycobacterium tuberculosis* (Mtb) immunodominant antigens CFP-10 and ESAT-6 and therefore were assumed to be Mtb uninfected.

Makerere University, Kampala, Uganda. Children from age 2-60 months hospitalized with lower respiratory infection (LRTI) from etiologies other than TB were recruited from Mulago Hospital Paediatric Wards. All children were HIV-negative and had no known recent TB contacts. Children were reassessed two months following enrollment to establish vital status and ensure clinical improvement. Following completion of the study, data from all participating children was reviewed by study investigators (DAL, CLL, SK) to confirm diagnosis of non-TB LRTI. Blood was drawn into citrate CPT tubes (BD) and processed per manufacturer's instructions to isolate PBMC within 24hr of collection, and PBMC subsequently cryopreserved. Adult participants were recruited from the National TB Treatment Center at Mulago Hospital, hospital staff, and the community surrounding Kampala, Uganda, between 2001 and 2014. Participants were HIV uninfected and included individuals with (tuberculin skin test, TST ≥ 10) or without (TST < 10 mm) evidence of Mtb infection. All had the absence of signs or symptoms of TB (prolonged cough, hemoptysis, fever, weight loss, and night sweats). Heparinized blood was collected for PBMC isolation by means of density gradient centrifugation.

Study approvals

349 The studies of all participants were conducted in accordance with the World's Medical
350 Association's Declaration of Helsinki guidelines. The studies from the Western Cape, South Africa
351 were approved by the Human Research Ethics Committee (HREC) of the University of Cape
352 Town. Written informed consent was obtained from parents or legal guardians of adolescents and
353 infants. Adolescents also provided written informed assent. The Institutional Review Board of
354 Oregon Health & Science University (Portland, Oregon) approved this study of participants from
355 Portland, OR. Written, informed consent was obtained from all adult participants and from a parent
356 or legal guardian of infants before enrollment. For participants from Kampala, Uganda, the
357 National Council for Science and Technology, HIV/AIDS Research Committee in Uganda, the
358 Institutional Review Board of Oregon Health & Sciences University (Portland, OR) and the
359 Institutional Review Board of Makerere University (Kampala, Uganda) approved this study.
360 Written, informed consent was obtained from all adult participants and from a parent or legal
361 guardian of infants and children before enrollment.

362 **Infection of antigen presenting cells**

363 A549 cells (ATCC CCL-185) were used as stimulators for direct ex vivo determination of
364 mycobacterial-reactive T cells. *Mycobacterium smegmatis* (strain mc^2155, ATCC) was grown to
365 late log phase and functionally titered in this assay to find the optimal volume of *M. smegmatis*
366 that elicited a strong response in an adult control donor but did not reduce the viability of the
367 antigen presenting cells. A549 cells were seeded in T25 flasks at 1.25e6 in 7.5ml of antibiotic free
368 media. After allowing cells to adhere for 3 hours, the flasks were infected with 31µl of *M.*
369 *smegmatis*. After 18 h, the cells were harvested and washed twice in RPMI/10% human serum
370 containing antibiotic (gentamicin) before being resuspended in RPMI/10% human serum
371 containing antibiotic (gentamicin).

372 **Flow cytometry assays**

373 To perform ICS, cryopreserved PBMC were thawed in the presence of DNAse,
374 resuspended, in 10% heat inactivated human serum with RPMI (Lonza) at a concentration of 2 x
375 10^7/ml. PBMC (2 x 10^6 cells/well) were stimulated with anti-CD28 (1 µg/ml) and anti-CD49d (1
376 µg/ml) (FastImmune, BD Biosciences) and 1e5 *M. smegmatis*-infected or uninfected A549 cells
377 in RPMI/10% Human Serum for 18 h at 37°C with 5% $C0_2$. During the last 12 h of this incubation,
378 Brefeldin-A (5 µg/ml) was added. PBMC incubated with uninfected A549 cells were used to assess
379 for background cytokine production. To determine the total functional capacity of T cells, PBMC
380 were incubated with uninfected A549 cells and PMA/Ionomycin (PMA, 20ng/ml, Sigma;
381 Ionomycin, 1µM, Sigma) for 3 hr. PBMC were then harvested and stained with MR1-5-OP-RU or
382 MR1-6FP tetramers (Corbett et al., 2014) (NIH Tetramer Core) at a 1:500 dilution for 45 minutes
383 at room temperature. All tetramers used were conjugated to R-phycoerythrin (PE) or Brilliant
384 Violet (BV) 421. After 45 minutes, an antibody cocktail containing LIVE/DEAD Fixable Dead
385 Cell Stain Kit (Thermo Fisher), and the surface antibodies listed in S1 Table were added for 30
386 minutes at 4°C. After washing, cells were fixed and permeabilized using Cytofix/Cytoperm (BD
387 Biosciences) per manufacturer's instructions. Cells were then stained for CD3 and TNF, then fixed
388 in 1% PFA. Acquisition was performed using a (Beckman Coulter) Cytoflex flow cytometer with

389 CytExpert software (BC). All flow cytometry data was analyzed using FlowJo software (TreeStar)
390 and Prism (Graphpad).

391 To perform cell surface staining for phenotyping MR1T cells, cryopreserved PBMC were
392 thawed as described above, and 1-2 x 10^6 PBMC were stained with MR1/5-OP-RU or MR1/6FP
393 tetramers at 1:500 for 45 minutes at room temperature. Cells were then subsequently stained with
394 an antibody cocktail containing LIVE/DEAD Fixable Dead Cell Stain Kit (Thermo Fisher), and
395 surface stained with the antibodies listed in S2-S4 Tables for 30 minutes at 4°C. Samples were
396 washed and fixed with 1% PFA. Acquisition of the US samples was performed using a Cytoflex
397 flow cytometer (Beckman) with CytExpert software (BC). For experiments with the Ugandan
398 samples, acquisition was performed on a BD LSRFortessa. For experiments performed at SATVI,
399 samples were acquired on a BD LSR-II flow cytometer configured with 4 lasers: solid state blue
400 (488nm; 100mW; 3 detectors), solid state violet (405nm; 25mW; 8 detectors), HeNe gas red
401 (635nm; 70mW; 3 detectors), and diode-pumped Coherent Compass yellow-green (532nm;
402 150mW; 8 detectors). Flow cytometric analysis was performed using FlowJo version 10.5.3
403 (Treestar, Ashland, OR, USA).

404 **Data analysis and Statistics**

405 Adjusted frequency (raw frequency of cytokine production following stimulation minus
406 the frequency of cytokine production in resting/unstimulated condition), was used to account for
407 the potential presence of background, or non-specific, responses. A positive cytokine response was
408 defined as the detection of at least 0.05% cytokine-positive T cells (following background
409 subtraction). Prism version 7 (GraphPad, La Jolla, CA, USA) was used for data analysis. A p-value
410 < 0.05 was considered as statistically significant.

411 To characterize phenotypic diversity within MR1T cell populations at the different ages
412 we performed t-Stochastic Neighbor Embedding (tSNE) on MR1-5-OP-RU tetramer$^+$ defined
413 CD3$^+$ T cells. Data from MR1-5-OP-RU tetramer$^+$ cells from all individuals across the age groups
414 were concatenated into a single FCS file to perform tSNE analysis in FlowJo. Equal event sampling
415 was not performed due to low events per individual in the cord blood and infant samples.
416 Clustering analysis was performed based on the expression of five surface markers (CD4, CD8,
417 TRAV1-2, CD26, and CD161). Parameter settings were fixed at 2000 iterations with a learning
418 rate (Eta) of 10 and perplexity 30, respectively (van der Maaten and Hinton, 2008).

Conflict of Interest statement

The authors declare that the research was conducted in the absence of any commercial or financial relationships that could be construed as a potential conflict of interest.

Author Contributions

GMS, AG, DML, TJS and DAL contributed to the conception and/or design of the work. GMS and AG are joint first authors. TJS and DAL jointly supervised the work. MN, HMK, SK, JK, CL, EN, MS, WAH, MH and TJS contributed to clinical activities. EN, WAH, MH, DML, DAL and TJS raised grants to fund the research. GMS, AG, MEC, MDN, RBD, DML, TJS and DAL substantially contributed to the acquisition, analysis or interpretation of data and drafting of the manuscript. All authors substantially contributed to revising and critically reviewing the manuscript for important intellectual content. All authors approved the final version of this manuscript to be published and agree to be accountable for all aspects of the work.

Funding

This project has been funded in whole or in part with Federal funds from the National Institutes of Allergy and Infectious Diseases, National Institutes of Health, Department of Health and Human Services, under grant no R01 AI04229 and contract HHSN272200900053C.

Work at SATVI was supported by Aeras, the National Institutes of Health Grant R01-AI087915 and R01-AI065653 and the European and Developing Countries Clinical Trial Partnership. Anele Gela was supported by a Postdoctoral Fellowship from the Claude Leon Foundation.

The funders had no role in study design, data collection and analysis, decision to publish, or preparation of the manuscript.

Acknowledgments

We would like to thank the participants who gave time and dedication to this health research; W. Henry Boom, LaShaunda Malone and Keith Chervenak, Case Western Reserve University; and Erin Merrifield, Department of Pediatrics, OHSU, for their contributions to this study.

The MR1 tetramer technology was developed jointly by Dr. James McCluskey, Dr. Jamie Rossjohn, and Dr. David Fairlie, and the material was produced by the NIH Tetramer Core Facility as permitted to be distributed by the University of Melbourne.

449 **References**

450 Ben Youssef, G., Tourret, M., Salou, M., Ghazarian, L., Houdouin, V., Mondot, S., et al. (2018).
451 Ontogeny of human mucosal-associated invariant T cells and related T cell subsets. *Journal*
452 *of Experimental Medicine* 215(2)**,** 459-479. doi: 10.1084/jem.20171739.

453 Chua, W.J., Truscott, S.M., Eickhoff, C.S., Blazevic, A., Hoft, D.F., and Hansen, T.H. (2012).
454 Polyclonal Mucosa-Associated Invariant T Cells Have Unique Innate Functions in
455 Bacterial Infection. *Infection and Immunity* 80(9)**,** 3256-3267. doi: 10.1128/Iai.00279-12.

456 Constantinides, M.G., Link, V.M., Tamoutounour, S., Wong, A.C., Perez-Chaparro, P.J., Han,
457 S.J., et al. (2019). MAIT cells are imprinted by the microbiota in early life and promote
458 tissue repair. *Science* 366(6464). doi: 10.1126/science.aax6624.

459 Corbett, A.J., Eckle, S.B.G., Birkinshaw, R.W., Liu, L.G., Patel, O., Mahony, J., et al. (2014).
460 T-cell activation by transitory neo-antigens derived from distinct microbial pathways.
461 *Nature* 509(7500)**,** 361-+. doi: 10.1038/nature13160.

462 Dusseaux, M., Martin, E., Serriari, N., Peguillet, I., Premel, V., Louis, D., et al. (2011). Human
463 MAIT cells are xenobiotic-resistant, tissue-targeted, CD161hi IL-17-secreting T cells.
464 *Blood* 117(4)**,** 1250-1259. doi: 10.1182/blood-2010-08-303339.

465 Fergusson, J.R., Smith, K.E., Fleming, V.M., Rajoriya, N., Newell, E.W., Simmons, R., et al.
466 (2014). CD161 Defines a Transcriptional and Functional Phenotype across Distinct Human
467 T Cell Lineages. *Cell Reports* 9(3)**,** 1075-1088. doi: 10.1016/j.celrep.2014.09.045.

468 Georgel, P., Radosavljevic, M., Macquin, C., and Bahram, S. (2011). The non-conventional
469 MHC class I MR1 molecule controls infection by Klebsiella pneumoniae in mice. *Mol*
470 *Immunol* 48(5)**,** 769-775. doi: 10.1016/j.molimm.2010.12.002.

471 Gherardin, N.A., Souter, M.N.T., Koay, H.F., Mangas, K.M., Seemann, T., Stinear, T.P., et al.
472 (2018). Human blood MAIT cell subsets defined using MR1 tetramers. *Immunology and*
473 *Cell Biology* 96(5)**,** 507-525. doi: 10.1111/imcb.12021.
474 Godfrey, D.I., Koay, H.F., McCluskey, J., and Gherardin, N.A. (2019). The biology and
475 functional importance of MAIT cells. *Nat Immunol* 20(9)**,** 1110-1128. doi:
476 10.1038/s41590-019-0444-8.
477 Gold, M.C., Cerri, S., Smyk-Pearson, S., Cansler, M.E., Vogt, T.M., Delepine, J., et al. (2010).
478 Human mucosal associated invariant T cells detect bacterially infected cells. *PLoS Biol*
479 8(6)**,** e1000407. doi: 10.1371/journal.pbio.1000407.
480 Gold, M.C., Eid, T., Smyk-Pearson, S., Eberling, Y., Swarbrick, G.M., Langley, S.M., et al.
481 (2013). Human thymic MR1-restricted MAIT cells are innate pathogen-reactive effectors
482 that adapt following thymic egress. *Mucosal Immunology* 6(1)**,** 35-44. doi:
483 10.1038/mi.2012.45.
484 Harriff, M.J., McMurtrey, C., Froyd, C.A., Jin, H.H., Cansler, M., Null, M., et al. (2018). MR1
485 displays the microbial metabolome driving selective MR1-restricted T cell receptor usage.
486 *Science Immunology* 3(25). doi: UNSP eaao2556
487 10.1126/sciimmunol.aao2556.
488 Kjer-Nielsen, L., Patel, O., Corbett, A.J., Le Nours, J., Meehan, B., Liu, L., et al. (2012). MR1
489 presents microbial vitamin B metabolites to MAIT cells. *Nature* 491(7426)**,** 717-723. doi:
490 10.1038/nature11605.
491 Koay, H.F., Gherardin, N.A., Enders, A., Loh, L., Mackay, L.K., Almeida, C.F., et al. (2016). A
492 three-stage intrathymic development pathway for the mucosal-associated invariant T cell
493 lineage. *Nature Immunology* 17(11)**,** 1300-1311. doi: 10.1038/ni.3565.

494 Koay, H.F., Godfrey, D.I., and Pellicci, D.G. (2018). Development of mucosal-associated
495 invariant T cells. *Immunology and Cell Biology* 96(6)**,** 598-606. doi: 10.1111/imcb.12039.
496 Kurioka, A., Ussher, J.E., Cosgrove, C., Clough, C., Fergusson, J.R., Smith, K., et al. (2015).
497 MAIT cells are licensed through granzyme exchange to kill bacterially sensitized targets.
498 *Mucosal Immunology* 8(2)**,** 429-440. doi: 10.1038/mi.2014.81.
499 Le Bourhis, L., Dusseaux, M., Bohineust, A., Bessoles, S., Martin, E., Premel, V., et al. (2013).
500 MAIT Cells Detect and Efficiently Lyse Bacterially-Infected Epithelial Cells. *Plos*
501 *Pathogens* 9(10). doi: ARTN e1003681
502 10.1371/journal.ppat.1003681.
503 Legoux, F., Bellet, D., Daviaud, C., El Morr, Y., Darbois, A., Niort, K., et al. (2019). Microbial
504 metabolites control the thymic development of mucosal-associated invariant T cells.
505 *Science* 366(6464)**,** 494-499. doi: 10.1126/science.aaw2719.
506 Lepore, M., Kalinicenko, A., Colone, A., Paleja, B., Singhal, A., Tschumi, A., et al. (2014).
507 Parallel T-cell cloning and deep sequencing of human MAIT cells reveal stable oligoclonal
508 TCR beta repertoire. *Nature Communications* 5. doi: ARTN 3866
509 10.1038/ncomms4866.
510 Lindestam Arlehamn, C.S., Lewinsohn, D., Sette, A., and Lewinsohn, D. (2014). Antigens for
511 CD4 and CD8 T cells in tuberculosis. *Cold Spring Harb Perspect Med* 4(7)**,** a018465. doi:
512 10.1101/cshperspect.a018465.
513 Marais, B.J., Gie, R.P., Schaaf, H.S., Hesseling, A.C., Enarson, D.A., and Beyers, N. (2006).
514 The spectrum of disease in children treated for tuberculosis in a highly endemic area.
515 *International Journal of Tuberculosis and Lung Disease* 10(7)**,** 732-738.

516 Marais, B.J., Gie, R.P., Schaaf, H.S., Hesseling, A.C., Obihara, C.C., Nelson, L.J., et al. (2004a).
517 The clinical epidemiology of childhood pulmonary tuberculosis: a critical review of
518 literature from the pre-chemotherapy era. *International Journal of Tuberculosis and Lung*
519 *Disease* 8(3)**,** 278-285.
520 Marais, B.J., Gie, R.R., Schaaf, H.S., Hesseling, A.C., Obihara, C.C., Starke, J.J., et al. (2004b).
521 The natural history of childhood intra-thoracic tuberculosis: a critical review of literature
522 from the pre-chemotherapy era. *International Journal of Tuberculosis and Lung Disease*
523 8(4)**,** 392-402.
524 Martin, E., Treiner, E., Duban, L., Guerri, L., Laude, H., Toly, C., et al. (2009). Stepwise
525 Development of MAIT Cells in Mouse and Human. *Plos Biology* 7(3)**,** 525-536. doi:
526 ARTN e1000054
527 10.1371/journal.pbio.1000054.
528 Meermeier, E.W., Laugel, B.F., Sewell, A.K., Corbett, A.J., Rossjohn, J., McCluskey, J., et al.
529 (2016). Human TRAV1-2-negative MR1-restricted T cells detect S-pyogenes and
530 alternatives to MAIT riboflavin-based antigens. *Nature Communications* 7. doi: ARTN
531 12506
532 10.1038/ncomms12506.
533 Meierovics, A., Yankelevich, W.J.C., and Cowley, S.C. (2013). MAIT cells are critical for
534 optimal mucosal immune responses during in vivo pulmonary bacterial infection.
535 *Proceedings of the National Academy of Sciences of the United States of America* 110(33)**,**
536 E3119-E3128. doi: 10.1073/pnas.1302799110.

537 Meierovics, A.I., and Cowley, S.C. (2016). MAIT cells promote inflammatory monocyte
538 differentiation into dendritic cells during pulmonary intracellular infection. *Journal of*
539 *Experimental Medicine* 213(12)**,** 2793-2809. doi: 10.1084/jem.20160637.
540 Paul K Sue, M.M., and Maite de la Morena (2018). "Immunologic Development and
541 Susceptibility to Infection.," in *Principles and Practice of Pediatric Infectious Diseases.*
542 *5th ed.,* ed. G.C.P. S. Sarah Long, M. Fischer.: Elsevier), p85-92.
543 Reantragoon, R., Corbett, A.J., Sakala, I.G., Gherardin, N.A., Furness, J.B., Chen, Z.J., et al.
544 (2013). Antigen-loaded MR1 tetramers define T cell receptor heterogeneity in mucosal-
545 associated invariant T cells. *Journal of Experimental Medicine* 210(11)**,** 2305-2320. doi:
546 10.1084/jem.20130958.
547 Sakala, I.G., Kjer-Nielsen, L., Eickhoff, C.S., Wang, X., Blazevic, A., Liu, L., et al. (2015).
548 Functional Heterogeneity and Antimycobacterial Effects of Mouse Mucosal-Associated
549 Invariant T Cells Specific for Riboflavin Metabolites. *J Immunol* 195(2)**,** 587-601. doi:
550 10.4049/jimmunol.1402545.
551 Seshadri, C., Thuong, N.T.T., Mai, N.T.H., Bang, N.D., Chau, T.T.H., Lewinsohn, D.M., et al.
552 (2017). A polymorphism in human MR1 is associated with mRNA expression and
553 susceptibility to tuberculosis. *Genes and Immunity* 18(1)**,** 8-14. doi: 10.1038/gene.2016.41.
554 Sharma, P.K., Wong, E.B., Napier, R.J., Bishai, W.R., Ndung'u, T., Kasprowicz, V.O., et al.
555 (2015). High expression of CD26 accurately identifies human bacteria-reactive MR1-
556 restricted MAIT cells. *Immunology* 145(3)**,** 443-453. doi: 10.1111/imm.12461.
557 Treiner, E., Duban, L., Bahram, S., Radosavljevic, M., Wanner, V., Tilloy, F., et al. (2003).
558 Selection of evolutionarily conserved mucosal-associated invariant T cells by MR1 (vol
559 422, pg 164, 2003). *Nature* 423(6943)**,** 1018-1018. doi: 10.1038/nature01700.

560 Tsukamoto, K., Deakin, J.E., Graves, J.A.M., and Hashimoto, K. (2013). Exceptionally high
561 conservation of the MHC class I-related gene, MR1, among mammals. *Immunogenetics*
562 65(2)**,** 115-124. doi: 10.1007/s00251-012-0666-5.
563 van der Maaten, L., and Hinton, G. (2008). Visualizing Data using t-SNE. *Journal of Machine*
564 *Learning Research* 9**,** 2579-2605.
565 Walker, L.J., Tharmalingam, H., and Klenerman, P. (2014). The Rise and Fall of MAIT Cells
566 with Age. *Scandinavian Journal of Immunology* 80(6)**,** 462-463. doi: 10.1111/sji.12237.
567 Wang, H.M., D'Souza, C., Lim, X.Y., Kostenko, L., Pediongco, T.J., Eckle, S.B.G., et al. (2018).
568 MAIT cells protect against pulmonary Legionella longbeachae infection. *Nature*
569 *Communications* 9. doi: ARTN 3350
570 10.1038/s41467-018-05202-8.
571

572 **Figure Legends**

573 **Figure 1. Frequencies of tetramer-defined MR1T cell and phenotypically defined MAIT cell**
574 **populations in peripheral blood from individuals of different ages.** PBMC or CBMC were
575 stained with a live/dead discriminator, antibodies to CD3, CD4, CD8, TRAV1-2, CD26, CD161,
576 and either the MR1-5-OP-RU or MR1-6FP tetramers. Live, $CD3^+$ lymphocytes were gated and the
577 frequencies of MR1-5-OP-RU^+ or TRAV1-$2^+CD26^+CD161^+$ cells as a percentage of $CD3^+$
578 lymphocytes were determined (gating strategy in Figure S2). **A**. Flow cytometry plots showing
579 $CD3^+$ T cell staining with MR1-5-OP-RU tetramer, MR1-6FP tetramer, TRAV1-2 or
580 CD26/CD161 of samples from a representative US adult, infant and neonate. **B.** Frequencies of
581 tetramer-defined ($CD3^+$MR1-5-OP-RU^+) and phenotypically-defined ($CD3^+$TRAV1-
582 $2^+CD26^+CD161^+$) MAIT cells in neonates, 10 week-old infants and adolescents from South Africa,
583 neonates, 12 month-old infants and adults from the United States and infants (0-2 years old),
584 children (2-5 years old) and adults from Uganda (all cohorts, *n*=10). Mann-Whitney u-tests were
585 used to test differences between groups. Horizontal lines depict the median and the error bars the
586 95% confidence interval. **C.** Relative proportions of median phenotypically-defined
587 ($CD3^+$TRAV1-$2^+CD26^+CD161^+$) MAIT cells that are MR1-5-OP-RU^+ (Blue) and MR1-5-OP-
588 RU^- (Red shades) for each age group at each site. In each doughnut chart the MR1-5-OP-RU^-
589 population is further divided into $CD8^+$, $CD8^+CD4^+$, $CD4^+$, and $CD8^-CD4^-$ populations.

590 **Figure 2. Functional analysis of MAIT cells in individuals of different ages.** PBMC or CBMC
591 from the US cohort were incubated overnight with *M. smegmatis*-infected A549 cells or uninfected
592 A549 cells and then stained with the MR1-5-OP-RU or MR1/6FP tetramers, followed by staining
593 with a live/dead discriminator and antibodies to TCRγδ, CD3, CD4, CD8, TRAV1-2, CD26 and
594 CD161. ICS was then performed and the cells stained for TNF. **A.** Dot plots showing representative
595 co-staining of live, $TCR\gamma\delta^-CD3^+$TRAV1-$2^+CD26^+CD161^+$ cells with MR1-5-OP-RU and TNF in
596 *M. smegmatis* stimulated or unstimulated samples. The gating strategy is shown in Figure S3.
597 Examples of the TNF response in a neonate, infant and adult are shown. **B.** Frequencies of
598 functional, phenotypically-defined ($CD3^+$TRAV1-$2^+CD26^+CD161^+$) MAIT cells that are MR1-5-
599 OP-RU^+ or MR1-5-OP-RU^- as a proportion of $CD3^+$ $TCR\gamma\delta^-$ T cells. Horizontal lines depict the
600 median and the error bars the 95% confidence interval. Wilcoxon-rank sum was used to test
601 differences within the same cohort.

602 **Figure 3. Phenotypic diversity of MR1T cells in individuals of different ages.** t-Distributed
603 stochastic neighbor embedding (tSNE) plots showing MR1-5-OP-RU tetramer-defined MR1T
604 cells (gating strategy in Figure S2) and the phenotypic clusters of MR1T cells identified in the
605 South African (SA) or United States (US) cohorts. Plots represent cells from 10 samples from each
606 age group. **A.** and **C.** The five clusters identified in both sites are shown in **A** (SA) and **C** (US).
607 **B.** and **D.** Dot plots colored by the relative expression level of each marker (CD4, CD8, TRAV1-
608 2, CD161 or CD26) in tetramer-defined MR1T cells for each age group in **B** (SA) and **D** (US).
609 Red = highest expression, blue = lowest expression. **E.** and **F.** The proportion of each cluster of
610 tetramer-defined MR1T cells by age group is shown in **E** (SA) and **F** (US). Horizontal lines depict
611 the median and the error bars the 95% confidence interval. Mann-Whitney u tests were used to test
612 differences between groups.

613 **Figure 4. Phenotypic analysis of functional MR1T cells at different ages.** PBMC or CBMC
614 from the US cohort were incubated overnight with *M. smegmatis*-infected A549 cells, uninfected
615 A549 cells, or uninfected A549 cells and PMA/ionomycin. All cells were then stained with the
616 MR1-5-OP-RU or MR1-6FP tetramers, followed by a live/dead discriminator and antibodies to
617 TCRγδ, CD3, CD4, CD8, TRAV1-2, CD26 and CD161. ICS was then performed and the cells
618 stained for TNF. Live, TCRγδ$^-$CD3$^+$MR1-5-OP-RU$^+$ cells were gated and the TNF$^+$ percentage
619 determined in both the *M. smegmatis* stimulated and unstimulated conditions. The gating strategy
620 is shown in Figure S3. **A.** Dot plots showing TNF expression by live, TCRγδ$^-$MR1-5-OP-RU$^+$
621 CD3$^+$ cells in the same representative neonate, infant and adult as Figure 2A. **B.** Background
622 subtracted frequencies of TNF$^+$ MR1-5-OP-RU$^+$ CD3$^+$ cells in response to *M. smegmatis*-infected
623 A549 cells as a percentage of total MR1/5-OP-RU$^+$ CD3$^+$ cells are shown. Mann-Whitney u-tests
624 were used to test differences between groups. **C.** Background subtracted frequencies of TNF$^+$
625 cells to PMA/ionomycin among different T cell subpopulations, 1) MR1T cells (CD3$^+$TCRγδ$^-$
626 MR1-5-OP-RU$^+$ cells); 2) γδ T cells (CD3$^+$TCRγδ$^+$MR1-5-OP-RU$^-$ cells); 3) CD8$^+$ T cells
627 (CD3$^+$TCRγδ$^-$MR1-5-OP-RU$^-$CD8$^+$ cells); and 4) CD4$^+$ T cells (CD3$^+$TCRγδ$^-$MR1-5-OP-RU$^-$
628 CD4$^+$ cells). Wilcoxon-rank sum was used to test differences within the same cohort. **D.** and **E.**
629 Frequencies of TNF$^+$TRAV1-2$^+$ MR1-5-OP-RU$^+$ CD3$^+$ and TNF$^+$TRAV1-2$^-$ MR1-5-OP-RU$^+$
630 CD3$^+$ cells in response to *M. smegmatis* infected A549 cells (**D**) or PMA/ionomycin stimulation
631 (**E**) minus the background frequencies of TNF$^+$TRAV1-2$^+$/- MR1-5-OP-RU$^+$ CD3$^+$ cells.
632 Wilcoxon-rank sum was used to test differences within the same cohort.

633 **Figure 5. Analysis of MR1T cell development by measuring maturation markers.** PBMC or
634 CBMC from the US were stained as in Figure 1 with the addition of an antibody to CD27. Live,
635 CD3$^+$MR1-5-OP-RU$^+$ cells (gating strategy in Figure S2) were gated for the maturation pattern of
636 S1, S2 and S3 described in (Koay et al., 2016). S1 = CD161$^-$CD27$^-$, S2=CD161$^-$CD27$^+$,
637 S3=CD161$^+$CD27$^{+/-}$. **A.** Gating of MR1T cells for S1, S2 and S3 in a representative neonate, infant
638 and adult. **B.** Frequencies of S1, S2, and S3 MR1T cells as a percentage of CD3$^+$ MR1-5-OP-RU$^+$
639 cells are shown for U.S. neonates, infants and adults. Bars represent the median and the error bars
640 the 95% confidence interval.

641 **Figure 6. Comparative phenotypic analysis of MR1T and non-MR1T cells or TRAV1-2$^+$ and**
642 **TRAV1-2$^-$ MR1T cells at different ages.** PBMC or CBMC from the US were stained as in Figure
643 1 with the addition of antibodies to either CD45RA (**A, B**), CCR7 (**C, D**), CD38 (**E, F**) or CD56
644 (**G, H**). The gating strategy is shown in Figure S2 and examples of the staining of each marker is
645 shown in Figure S4. Frequencies of cells expressing each marker in non-MR1T cells (CD3$^+$MR1-
646 5-OP-RU$^-$) or MR1T cells (CD3$^+$MR1-5-OP-RU$^+$) in each age group (**A, C, E, G**). The frequency
647 of each marker expressed in TRAV1-2$^+$ or TRAV1-2$^-$ MR1T cells is shown in each age group (**B,**
648 **D, F, H**). The median and 95% confidence intervals are shown in each graph. When the 95%
649 confidence intervals do not overlap between conditions, those conditions are considered
650 statistically significant.

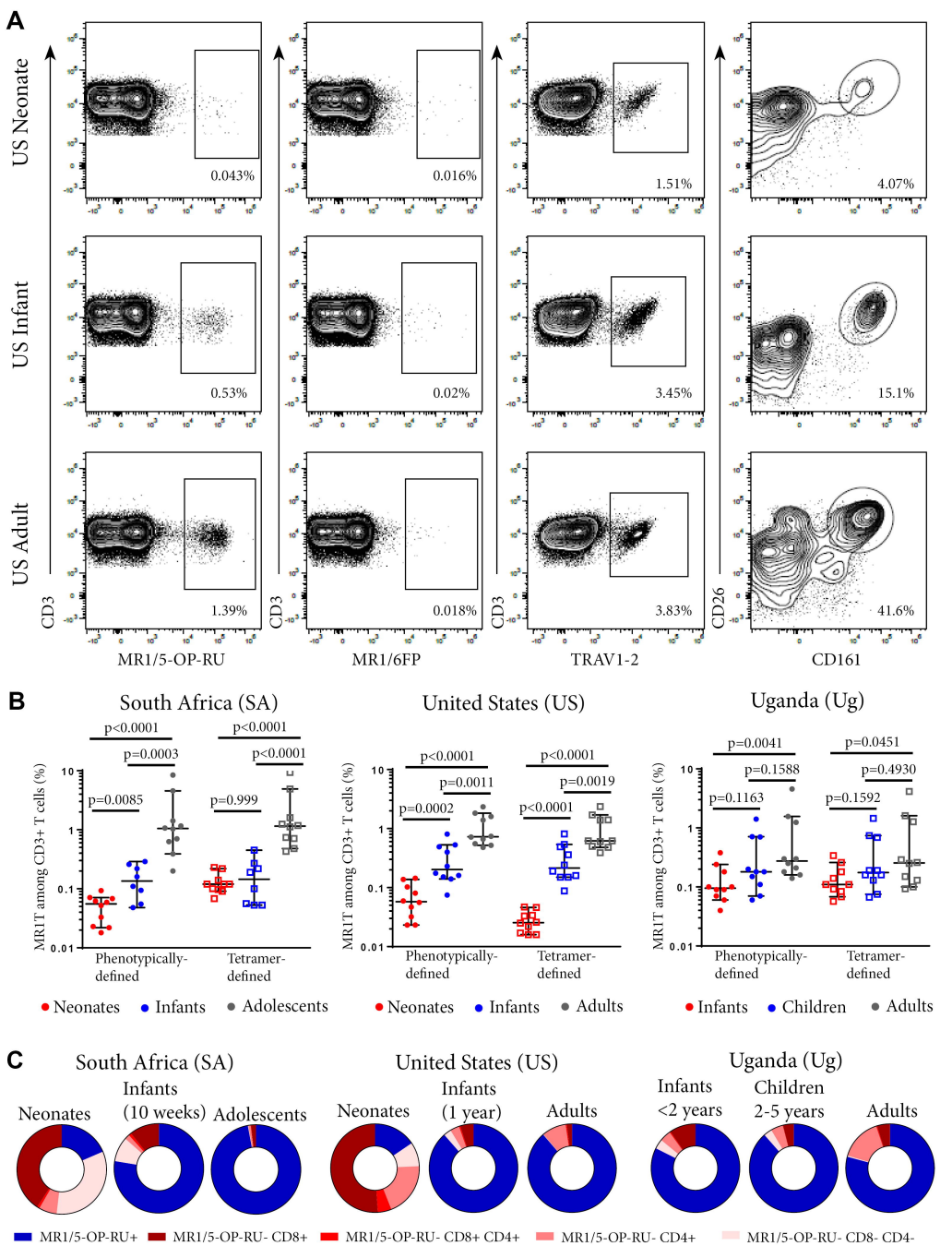
A
US Neonate
US Infant
US Adult
0.043%
0.016%
1.51%
4.07%
0.53%
0.02%
3.45%
15.1%
1.39%
0.018%
3.83%
41.6%
CD3
MR1/5-OP-RU
MR1/6FP
TRAV1-2
CD26
CD161
B
South Africa (SA)
United States (US)
Uganda (Ug)
MR1T among CD3+ T cells (%)
p<0.0001
p=0.0003
p=0.0085
p<0.0001
p<0.0001
p=0.999
p<0.0001
p<0.0001
p=0.0011
p=0.0002
p<0.0001
p<0.0001
p=0.0019
p=0.0041
p=0.1588
p=0.1163
p=0.0451
p=0.4930
p=0.1592
Phenotypically-defined
Tetramer-defined
Neonates
Infants
Adolescents
Adults
Children
C
Neonates
Infants (10 weeks)
Adolescents
Infants (1 year)
Infants <2 years
Children 2-5 years
MR1/5-OP-RU+
MR1/5-OP-RU- CD8+
MR1/5-OP-RU- CD8+ CD4+
MR1/5-OP-RU- CD4+
MR1/5-OP-RU- CD8- CD4-

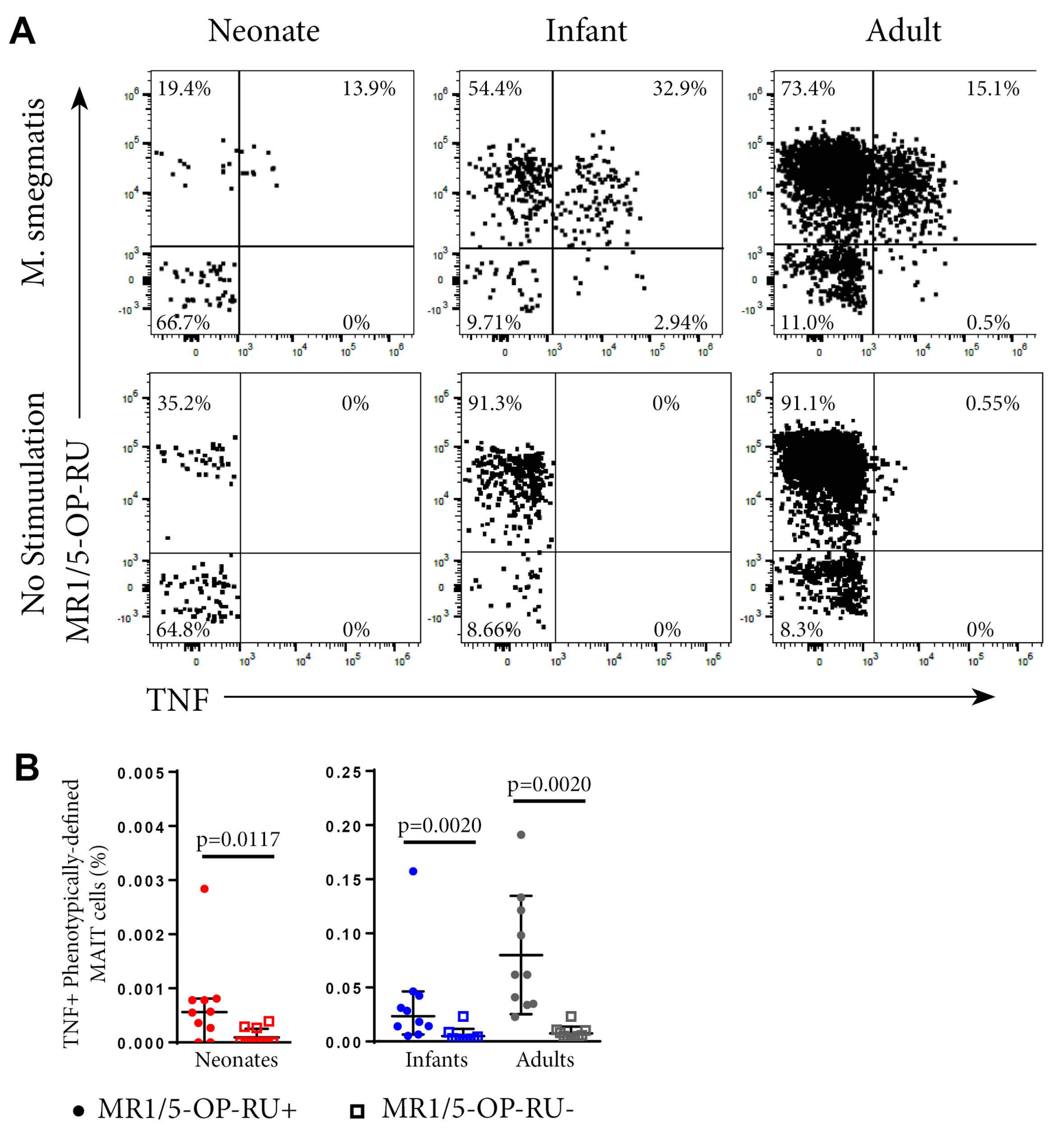
A
Neonate
Infant
Adult
M. smegmatis
No Stimulation
MR1/5-OP-RU
19.4%
13.9%
66.7%
0%
54.4%
32.9%
9.71%
2.94%
73.4%
15.1%
11.0%
0.5%
35.2%
0%
64.8%
0%
91.3%
0%
8.66%
0%
91.1%
0.55%
8.3%
0%
TNF
B
TNF+ Phenotypically-defined MAIT cells (%)
p=0.0117
p=0.0020
p=0.0020
Neonates
Infants
Adults
MR1/5-OP-RU+
MR1/5-OP-RU-

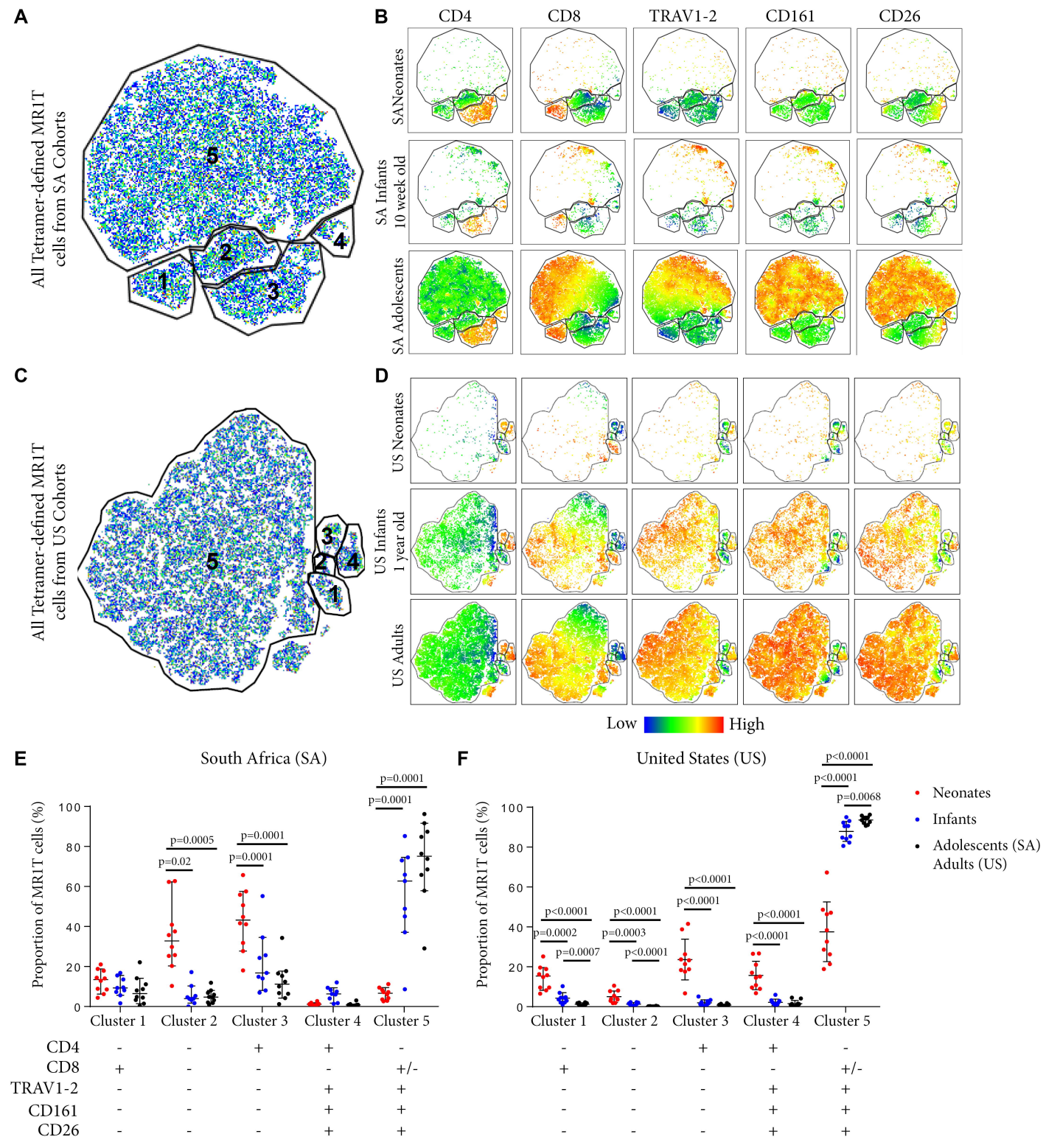
A
All Tetramer-defined MR1T cells from SA Cohorts
1
2
3
4
5
B
CD4
CD8
TRAV1-2
CD161
CD26
SANeonates
SA Infants 10 week old
SA Adolescents
C
All Tetramer-defined MR1T cells from US Cohorts
1
2
3
4
5
D
US Neonates
US Infants 1 year old
US Adults
Low
High
E
South Africa (SA)
Proportion of MR1T cells (%)
Cluster 1
Cluster 2
Cluster 3
Cluster 4
Cluster 5
p=0.02
p=0.0005
p=0.0001
p=0.0001
p=0.0001
p=0.0001
F
United States (US)
Proportion of MR1T cells (%)
Cluster 1
Cluster 2
Cluster 3
Cluster 4
Cluster 5
p<0.0001
p=0.0002
p=0.0007
p<0.0001
p=0.0003
p<0.0001
p<0.0001
p<0.0001
p<0.0001
p<0.0001
p<0.0001
p<0.0001
p=0.0068
Neonates
Infants
Adolescents (SA)
Adults (US)
CD4 - - + + -
CD8 + - - - +/-
TRAV1-2 - - - + +
CD161 - - - + +
CD26 - - - + +
- - + + -
+ - - - +/-
- - - + +
- - - + +
- - - + +

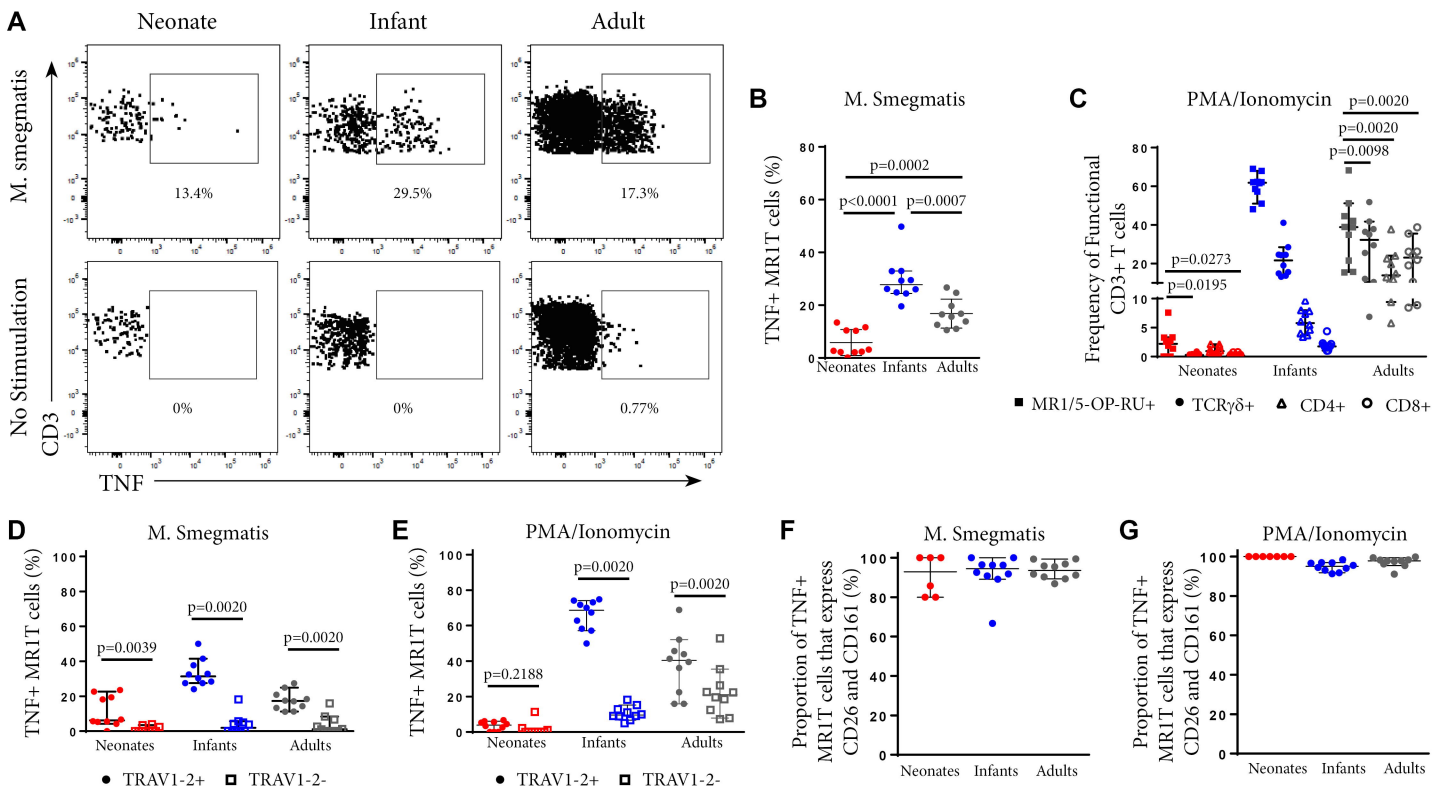
A
Neonate
Infant
Adult
M. smegmatis
No Stimulation
CD3
TNF
13.4%
29.5%
17.3%
0%
0%
0.77%
B
M. Smegmatis
TNF+ MR1T cells (%)
p=0.0002
p<0.0001
p=0.0007
Neonates
Infants
Adults
C
PMA/Ionomycin
Frequency of Functional CD3+ T cells
p=0.0020
p=0.0020
p=0.0098
p=0.0273
p=0.0195
Neonates
Infants
Adults
MR1/5-OP-RU+
TCRγδ+
CD4+
CD8+
D
M. Smegmatis
TNF+ MR1T cells (%)
p=0.0039
p=0.0020
p=0.0020
Neonates
Infants
Adults
TRAV1-2+
TRAV1-2-
E
PMA/Ionomycin
TNF+ MR1T cells (%)
p=0.2188
p=0.0020
p=0.0020
Neonates
Infants
Adults
TRAV1-2+
TRAV1-2-
F
M. Smegmatis
Proportion of TNF+ MR1T cells that express CD26 and CD161 (%)
Neonates
Infants
Adults
G
PMA/Ionomycin
Proportion of TNF+ MR1T cells that express CD26 and CD161 (%)
Neonates
Infants
Adults

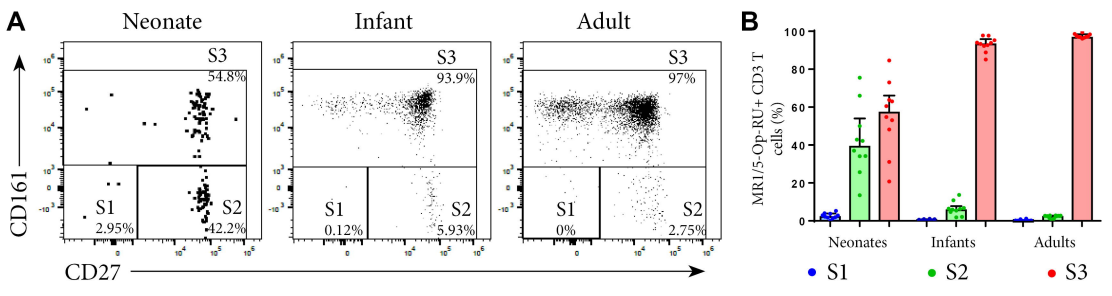
A
Neonate
Infant
Adult
S3
54.8%
S1
2.95%
S2
42.2%
S3
93.9%
S1
0.12%
S2
5.93%
S3
97%
S1
0%
S2
2.75%
CD161
CD27
B
MR1/5-Op-RU+ CD3 T cells (%)
Neonates
Infants
Adults
S1
S2
S3

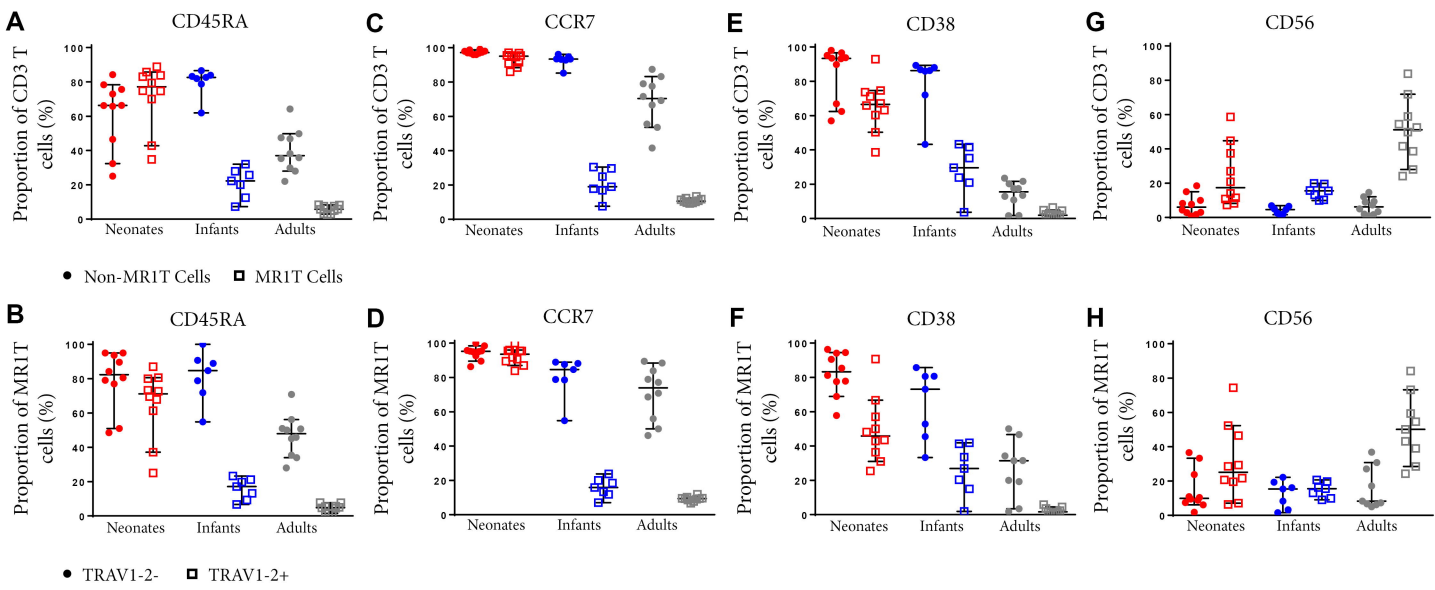
A
CD45RA
Proportion of CD3 T cells (%)
Neonates
Infants
Adults
C
CCR7
E
CD38
G
CD56
Non-MR1T Cells
MR1T Cells
B
CD45RA
Proportion of MR1T cells (%)
D
CCR7
F
CD38
H
CD56
TRAV1-2-
TRAV1-2+